When good species have porous boundaries: weak reproductive isolation and extensive gene flow between *Mimulus glaucescens* and *M. guttatus* in northern California.

C. T. Ivey[1*], N. M. Habecker[1], J. P. Bergmann[1], J. Ewald[1], and J. M. Coughlan[2]

[1]Department of Biological Sciences, California State University, Chico, CA, 95929-0515

[2]Department of Ecology and Evolutionary Biology, Yale University, 165 Prospect St., New Haven, CT, 06520

*correspondence: ctivey@csuchico.edu

Running title: Good species with porous boundaries

ACKNOWLEDGEMENTS

We acknowledge the indigenous native peoples of California as the traditional stewards of the ecosystems studied for this project. K. M. Kay, J. M. Sobel, and the A. L. Sweigart lab commented on the manuscript; L. S. Kimsey of the University of California, Davis Bohart Museum identified floral visitors; L. Bergmann, C. Bruns, T. Devine, J. Habecker, M. Patterson, and A. Pokrzywinski helped in the field and greenhouse; K. A. Blee, K. F. Gorman, C. Hatfield, J. M. Sobel, D. G. Miller, and K. A. Schierenbeck provided advice and suggestions; and the Big Chico Creek Ecological Reserve, California Botanical Society, California Native Plant Society, Chico State Center for Water and the Environment, Friends of the Chico State Herbarium, Northern California Botanists, and the Vesta Holt Field Research Award provided financial support.

AUTHOR CONTRIBUTIONS

CTI conceived and designed experiments, collected and analysed data; NMH, JPB, and JE designed experiments and collected data; JMC analysed data; all authors contributed to writing the manuscript.

DATA ACCESSIBILITY

Data used to characterize reproductive isolation available on Figshare: https://figshare.com/articles/dataset/Monkeyflower_reproductive_boundaries_-_glaucescens_and_guttatus/20407368

Abstract:

Barriers to reproduction are often how progress in speciation is measured. Nonetheless, a key unresolved question is the extent to which reproductive barriers diminish gene flow in incipient species in nature. The Sierra Nevada foothill endemic *Mimulus glaucescens* and the widespread *M. guttatus* are considered to be distinct species based on contrasting vegetative traits, but barriers to reproduction are not readily apparent, although these species are not known to hybridize in nature. To explore boundaries between taxa, we examined 15 potential reproductive barriers between species in a Northern California area of broad sympatry. Most barriers, with the exception of ecogeographic isolation, were weak, and total isolation for each species was estimated to be incomplete. Population genomic analyses of range-wide and broadly sympatric accessions revealed that gene flow between these taxa is common across the range, and rampant within areas of sympatry. Thus, despite fairly strong ecological differentiation - which may be involved in maintenance of vegetative differences - ecological isolation is a weak barrier to gene flow in this system. This work underscores the value of combining classical measures of reproductive isolation with estimates of natural gene flow for studies of speciation in natural communities.

Keywords: speciation continuum, reproductive isolation, *Mimulus*, introgression, gene flow, ecotype

INTRODUCTION

Species boundaries are often considered to be maintained by reproductive barriers that limit interbreeding (Mayr 1942). The effectiveness of these barriers at limiting gene flow typically varies (Lowry et al. 2008a; Widmer et al. 2009; Baack et al. 2015), and in many cases boundaries are established only through multiple barriers in combination, no one of which is sufficient to preclude all gene flow (Ramsey et al. 2003; Kay 2006; Ostevik et al. 2016; Christie and Strauss 2019). Species boundaries also can be maintained with few barriers to reproduction if opposing selection is sufficiently strong (Via 2009; DiVittorio et al. 2020). However, interbreeding can itself alter the strength of reproductive barriers, either positively or negatively (Servedio and Kirkpatrick 1997; Runemark et al. 2019). Moreover, the pace and sequence of barrier evolution appears to be quite variable (Widmer et al. 2009; Baack et al. 2015; Coughlan and Matute 2020), and in some cases results in apparently stable partial isolation, in which some gene flow is routine (Stankowski and Ravinet 2021).

As a consequence, some authors have suggested that boundaries between species or populations are best regarded as falling along a continuum, with panmixia and complete isolation at the extremes, and the strength of reproductive barriers between two populations defining their position on the continuum (Merill et al. 2011; Powell et al. 2013; Feder et al. 2014; Harrison and Larson 2014; Christie and Strauss 2019; Stankowski and Ravinet 2021). In this context, estimates of reproductive isolation between species or populations might be expected to inform predictions about genetic divergence as well as the likelihood of ongoing gene exchange. Estimates of barrier strength, however, are not always reliable indicators of gene flow. Sambatti et al. (2012), for example, estimated reproductive isolation between *Helianthus annuus* and *H. petiolaris* to exceed 0.999, based on multiple potential barriers, but nonetheless found extensive introgression between species, based on sampling multiple

96 nuclear loci. De La Torre et al. (2014) similarly found extensive admixture between two
97 *Picea* species based on genome-wide SNP panels, but also found evidence that adaptation to
98 different climatic conditions helped maintain species integrity. Finally, although prezygotic
99 reproductive isolation has been estimated to exceed 0.99 between the recently diverged
100 *Mimulus guttatus* and *M. nasutus* (Martin and Willis 2006), introgression appears common
101 between these taxa (Brandvain et al. 2014; Kenney and Sweigart 2016). Thus, interpretation
102 of estimates of reproductive isolation with respect to species boundaries benefits from more
103 direct estimates of gene flow and introgression based on genomic sampling.

104 Progress in understanding the evolution of reproductive isolation and patterns of
105 speciation has often come from studies of groups of related taxa (Coyne and Orr 1989; Moyle
106 et al. 2004; Owens and Rieseberg 2013; Christie and Strauss 2018; Coughlan and Matute
107 2020). One such group includes the diverse wildflower genus *Mimulus* (Wu et al. 2008;
108 Twyford et al. 2015; Nelson et al. 2021; note that some taxa were placed into other genera by
109 Barker et al. [2012], but we herein follow Lowry et al. [2019] in the use of *Mimulus* given the
110 lack of a well-resolved phylogeny). Comparative studies involving *Mimulus* have suggested
111 habitat divergence, mating system differentiation, or shifts in floral traits associated with
112 pollination may be common during speciation (Grossenbacher and Whittall 2011;
113 Grossenbacher et al. 2014; Sobel et al. 2014). As divergence proceeds, however, post-
114 pollination barriers appear to increase in strength (Ferris et al. 2014; Coughlan et al. 2020;
115 Sandstedt et al. 2021; Joffard et al. 2021). Introgression has also been a salient feature during
116 speciation in *Mimulus* (Brandvain et al. 2014; Kenny and Sweigart 2016; Nelson et al. 2021).
117 Within the adaptive radiation of *Mimulus* section *Erythranthe*, for example, extensive
118 ancestral and recent introgression has been documented, even between taxa with strong
119 reproductive barriers, which underscores the importance of natural selection in boundary
120 maintenance (Nelson et al. 2021).

121 Many of the *Mimulus* taxa studied to date have relatively conspicuous contrasts in
122 distribution, habitat, floral traits, or mating system that result in barriers to reproduction. In
123 contrast, the taxa studied herein, *M. glaucescens* and *M. guttatus*, have few apparent
124 constraints on gene exchange (see below). Taxonomists, however, have treated them as
125 distinct species based on marked contrasts in vegetative morphology (Fig. 1; Baldwin et al.
126 2012; Barker et al. 2012; Nesom 2012), and natural hybrids are not commonly observed
127 (Vickery 1964). Here, we characterize 15 potential reproductive barriers and use whole-
128 genome resequencing to estimate barrier strength and compare patterns of reproductive
129 isolation with patterns of population genetic structure, divergence, and introgression to better
130 understand boundaries between these taxa. Our results contribute to understanding how
131 reproductive barriers relate to introgression and illuminate the speciation process in recently
132 diverged taxa.
133
134 METHODS
135
136 Study system
137 The genus *Mimulus* (family Phrymaceae) is a diverse group of at least 180 plant
138 species (Grant 1924; Beardsley et al. 2004; Barker et al. 2012) that has been a focus for
139 studies of evolution and speciation (Schemske and Bradshaw 1999; Martin and Willis 2007;
140 Lowry et al. 2008b; Wu et al. 2008; Sobel 2014; Twyford et al. 2015; Nelson et al. 2021;
141 Sandstedt et al. 2021). Some taxa within section *Simiolus*, which includes *M. guttatus*, have
142 been taxonomically problematic (Munz 1959; Hickman 1993; Nesom 2012) and likely
143 represent multiple recently evolved lineages (Beardsley et al. 2004; Sweigart and Willis
144 2003; Lowry et al. 2008b; Barker et al. 2012). The similar *M. glaucescens*, however, has been
145 considered distinct from *M. guttatus* based on vegetative characters (Baldwin et al. 2012;

146 Nesom 2012). Nesom (2012) described *M. glaucescens* as "clearly defined" in a recent
147 treatment of the section. *Mimulus glaucescens* has peduncular bracts that are perfoliate to
148 connate, glabrous, distinctly glaucous, and with entire margins, whereas the peduncular
149 bracts of *M. guttatus* are generally distinct, bearing trichomes that are often glandular, lacking
150 in glaucousness, and with margins that are often dentate (Fig. 1; Baldwin et al. 2012).
151 Phylogenies suggest the two are closely related, and possibly sister taxa (Beardsley et al.
152 2004; Lowry et al. 2019). Both species are mixed-mating herbs, flower during the spring,
153 occur in similar habitats, and are $n = 14$ (Vickery 1978; Ritland and Ritland 1989; Baldwin et
154 al. 2012). *Mimulus glaucescens* is endemic to a few counties within northern California,
155 whereas the broad western North American range of *M. guttatus* wholly overlaps that of *M.*
156 *glaucescens* (Baldwin et al. 2012; Nesom 2012). Within the range of *M. glaucescens*, *M.*
157 *guttatus* is found on non-serpentine soils (C. T. Ivey, pers. obs.), although it occurs on
158 serpentine elsewhere (Selby and Willis 2018; Sianta & Kay 2021). In contrast, *M.*
159 *glaucescens* occurs on both serpentine and non-serpentine soils (Nesom 2012). Populations in
160 the current study were from non-serpentine sites unless otherwise noted. Previous work using
161 few maternal lines reported reduced hybrid seed set and F_1 fertility between *M. glaucescens*
162 and *M. guttatus* (Vickery 1964). Otherwise, little appears to be known about what limits
163 hybridization between these taxa.
164
165 <u>Pre-pollination barriers</u>
166 To characterize the importance of pre-pollination barriers to species boundaries,
167 geographical distribution, local habitat, flowering phenology, floral visitor behavior, and
168 floral morphology were compared between species. Habitat associated with each species was
169 modelled using 2512 georeferenced collection records from the Global Biodiversity
170 Information Facility, which were filtered after download (GBIF; 2194 *M. guttatus* records*:*

171 https://doi.org/10.15468/dl.ywy9s3 and 318 *M. glaucescens:*
172 https://doi.org/10.15468/dl.r93avz; see Supplemental Methods and Results) and
173 environmental data including primary and secondary geological substrates, elevation, and 19
174 bioclimatic variables (https://www.worldclim.org/), all standardized to a resolution of 2.5
175 minutes. Species distribution models were constructed using MaxEnt by sampling locations
176 of collection records as well as 1000 randomly located background samples from across the
177 geographic extent to create pseudo-absence data (Coughlan et al. 2021). Models were
178 computed separately for each species, and reproductive isolation was inferred based on the
179 number of shared and unshared pixels in the map following equation RI_{4C} from Sobel and
180 Chen (2014) (see Supplemental Methods and Results).
181 In addition, local-scale habitat characteristics were measured for each species within a
182 6 km^2 region of sympatry along Butte Creek within Butte county California. Within each of
183 15 populations (*M. glaucescens* = 9; *M. guttatus* = 6), slope, percent shade cover, percent
184 vegetative cover, percent bare ground, percent debris, and percent standing water was
185 measured for each of 8-10 randomly chosen plants (*sensu* Li et al. 2018). Scores of the first
186 two principal components of the combined data were compared between species using a
187 mixed-model ANOVA with species as the fixed effect and population as the random effect.
188 Flowering phenology was compared between species within a flowering season for
189 four populations of each species occurring within a 2 km^2 region along Butte Creek (Table
190 S1). The number of flowering plants was recorded once each week from mid-March (when
191 no plants were flowering) until early August (after all flowering had stopped). Flowering
192 plant numbers were compared between species using a repeated measures model in which
193 plant species, day of observation, and their interaction were fixed effects, and population pair
194 was a random effect. The day of observation was the repeated effect with population as the
195 subject.

196 The behavior of floral visitors was compared between species using experimental
197 mixed-species arrays placed near natural populations of each species (Table S1). Each array
198 consisted of 18 plants of each species (36 total) in 9 cm^2 pots arranged into a 6 x 6 grid at 0.5
199 m spacing. Each plant in the array had a single first-day flower open during observations.
200 Arrays were observed between 0900 and 1500 for 1 hr intervals (total 67 hr) during which the
201 visitor taxon and sequence of visited plants was recorded. The likelihood of floral visitors
202 moving conspecifically (response = 0) vs. heterospecifically (1) was compared for visitors
203 foraging on each species using a generalized linear mixed model with a binomial error
204 distribution. Fixed effects included the plant species from which the visitor moved, site
205 location, and their interaction. Random effects included visitor taxon (Table S2) and the
206 observation.
207 First-day floral morphology was compared between species using greenhouse-grown
208 plants reared from open-pollinated seeds collected in four populations of each species (Table
209 S1). Corolla width at the widest point, corolla tube width at distal opening, anther length,
210 pistil length, and herkogamy were measured to the closest mm for 120 first-day flowers (*M.*
211 *glaucescens* $n = 73$; *M. guttatus* $n = 47$), and scores of the first two principal components
212 based on family mean values were compared between species using a mixed-model ANOVA
213 with species as the fixed effect and population as the random effect (see Supplemental
214 Methods and Results).
215
216 Post-pollination barriers
217 To characterize the importance of post-pollination barriers to species boundaries,
218 pollen-pistil interactions, seed number, seed germination, and several measures of post-
219 germination performance were measured following controlled hand-pollinations of
220 emasculated flowers within species (both within- and between-populations) and between

221 species. Hand-pollinations were performed on plants reared in the greenhouse from open-
222 pollinated seeds collected from at least two populations of each species within the Butte
223 Creek watershed (Table S1).

224 To evaluate pollen-pistil interactions, pollen adhesion, pollen germination, and pollen-
225 tube growth rate (PTGR) were compared among types of hand-pollinations (*sensu* Kay
226 2006). The success of pollen adhesion was compared using a modification of Zinkl et al.
227 (1999). A known number of pollen grains was applied to first-day stigmas (*M. glaucescens n*
228 = 42; *M. guttatus n* = 53), which were then vortexed in a phosphate-Tween-20 solution,
229 centrifuged for 60 sec at 7200 rpm, and fixed in 9:1 ethanol:glacial acetic acid for 24 hr
230 before staining with basic fuchsin and viewing at 100x to record number of adhered pollen
231 grains. Pollen germination was observed in styles (*M. glaucescens n* = 61; *M. guttatus n* = 56)
232 that were excised 6-12 hr following hand-pollination, fixed and stained in decolorized 0.1%
233 aniline blue before viewing at 100x under epifluorescence. The number of pollen tubes in
234 styles and number of pollen grains on stigmas was recorded. Pollen tube growth rate was
235 observed in styles (*M. glaucescens n* = 25; *M. guttatus n* = 42) that were excised five minutes
236 after hand-pollination and placed onto enriched 1% agar. Style length was measured to the
237 nearest 0.1 mm using a dissection microscope fitted with an ocular micrometer and the time
238 in min for pollen tubes to emerge from the style was recorded (see Supplemental Methods
239 and Results).

240 Seed number was recorded for individual fruits resulting from hand-pollinations of
241 emasculated flowers (*M. glaucescens n* = 119; *M. guttatus n* = 185) using digital images
242 following Ivey and Carr (2012). Sixty fruits from each species were randomly chosen, and 20
243 seeds from each were scored for germination (number of seedlings) two weeks after sowing
244 into 100 cm^2 pots. One randomly chosen seedling from each fruit was grown to maturity, and
245 the number of days until the first flower opened (DFF) was scored to indicate development.

246 In addition, ovule number and pollen viability were scored from the first open flower
247 following Carr and Dudash (1997). After 59 days, total number of flowers was recorded, and
248 all above-ground biomass was dried to constant mass at 55º C before weighing to nearest mg.
249 Post-pollination traits were compared using mixed-model ANOVA that included
250 hand-pollination category (within-population, between-population conspecific, and
251 heterospecific), the species of pollen recipient, and their interaction as fixed effects, whereas
252 random effects included the population identities of pollen donor and pollen recipient.
253 Additional details about models used for each trait can be found in Supplemental Methods
254 and Results.
255
256 Reproductive isolation
257 Reproductive isolation was estimated for each of the potential barriers above where
258 possible, following Sobel and Chen (2014). To provide context for interpreting estimates of
259 isolation between species, estimates of isolation were calculated between populations within
260 each species as well (Table S3). Total reproductive isolation was estimated from all barriers
261 using equation RI_{4E} from Sobel and Chen (2014). Stability of the estimates was evaluated by
262 constructing 95% confidence intervals for individual barriers as well as total isolation using
263 10,000 bootstrap replicates except in the case of ecogeographic isolation in which we used
264 1,000 bootstraps for computational efficiency (*sensu* Ostevik et al. 2016; Christie and Strauss
265 2019).
266
267 Genomic analyses
268 We paired previously published whole-genome re-sequencing data (Brandvain et al.
269 2014, Puzey et al. 2018, Coughlan et al. 2020, Coughlan et al. 2021) with new whole-genome
270 re-sequencing data described herein to assess taxonomic relationships, patterns of population

271 genetic structure, and the presence of introgression between *M. guttatus* and *M. glaucescens*
272 (See Table S4 for sample details). In total, we leverage data from 75 accessions representing
273 10 named species across the *M. guttatus* species complex plus a single accession of *M.*
274 *dentilobus* as an outgroup. For the newly described whole-genome re-sequencing data, we
275 followed protocols described elsewhere for sample preparation, sequencing, and preparation
276 of VCF files (e.g. Coughlan et al. 2020, Coughlan et al. 2021; see Supplemental Methods for
277 details).

278 *Phylogenetic relationships*: To assess phylogenetic relationships among named
279 members of the *M. guttatus* species complex we inferred a Maximum Likelihood (ML)
280 phylogeny as well as 1,000 ultrafast bootstraps using IQtree V2.0.3 (Nguyen et al. 2015) with
281 a TVM+F+R4 model, which IQtree identified as the best fitting model based on both AIC
282 and BIC. For this analysis, we filtered the VCF file to include sites in which 72 of the 75
283 accessions were genotyped (~95% of accessions), which resulted in 195,771 sites, 146,697 of
284 which were parsimony informative. We also performed principal components analyses on
285 genome-wide data using PCANGSD (Korneliussen et al. 2014) for all members of the
286 complex (Fig. S1) as well as just *M. guttatus* and *M. glaucescens,* to evaluate whether named
287 species correspond to genetically distinct clusters. We furthered this analysis by performing
288 K-means clustering analysis using both PCANGSD (in which K is identified as the number of
289 significant PCs +1) and more traditional K-means clustering analyses using NGSAdmix
290 (Skotte et al. 2013), in which we determined the best K by performing 10 replicate runs at Ks
291 1-7, then using CLUMPAK (Kopelman et al. 2015) to identify the best value of K. To
292 perform both PCANGSD and NGSADMIX analyses with only *M. glaucescens* and *M.*
293 *guttatus*, we generated a genotype likelihood file to include sites which contained data for 31
294 (out of a total of 34) individuals, a minimum mapping quality of 30, and a minimum base

295 quality of 20, which resulted in a final dataset including 13,827,721 sites. In both cases, K=3
296 was optimal, so we restricted subsequent analyses to the results from PCANGSD.
297 *Divergence, differentiation, and diversity*: We used *Pixy* to calculate divergence,
298 differentiation, and diversity (D_{XY}, F_{ST}, and π, respectively; Korunes & Samuk 2021) on 4-
299 fold degenerate synonymous sites for all 11 taxa included herein (Northern and Southern *M.*
300 *guttatus* clades were treated as distinct taxa for these analyses). For this analysis, the VCF
301 described above was curated to include only 4-fold degenerate synonymous sites (from
302 Brandvain et al. 2014, Coughlan et al. 2020), for the 14 main scaffolds of the *M. guttatus*
303 reference genome (corresponding to the 14 chromosomes in this group). We used the default
304 filtering expressions in *Pixy* (DP>=10, RGQ>=20 for invariant sites; DP>=10, GQ>=20,
305 RGQ>=20 for variant sites), and calculated D_{XY}, F_{ST}, and π in 500KB windows before
306 averaging all windows for genome-wide values (Table S5).
307 *Evidence for introgression*: We used Dsuite to assess Patterson's D (i.e. ABBA-
308 BABA statistics; Malinsky et al. 2021) for all possible trios of all individual genomes of
309 Northern *M. guttatus* (see Results for distinction of Northern *M. guttatus* versus Southern *M.*
310 *guttatus*) and *M. glaucescens*, given the ML phylogeny produced using IQtree. Our aims in
311 this analysis were first, to assess evidence for introgression between Northern *M. guttatus* and
312 *M. glaucescens*. Second, if significant introgression was inferred, we sought to compare the
313 magnitude of introgression between sympatric accessions of *M. glaucescens* and *M. guttatus,*
314 vs. allopatric accessions. Greater introgression between sympatric samples would be
315 indicative of ongoing gene flow, as opposed to historic gene flow or more complex patterns
316 of species bifurcation. To assess introgression we used a standard Jack-knifing procedure on
317 all Patterson's D statistics, with Bonferroni correction for multiple comparisons to determine
318 if any pairs of *M. guttatus* and *M. glaucescens* genomes exhibited significant introgression.
319 To assess whether introgression was stronger between sympatric accessions, we constructed a

320 linear mixed model with f_G (the proportion of the genome that has experienced introgression;
321 Malinksy *et al.* 2021) as the response variable, distribution type (whether *M. guttatus* sample
322 was sympatric or allopatric) as fixed effect, and the individual identities of P1 in each trio as
323 random effects. We assessed significance of the fixed effect (i.e. distribution type) with an
324 ANOVA using a Wald's χ^2.

325
326
327 RESULTS

328

329 Species distribution modeling

330 The predicted distribution of *M. glaucescens* was centered on an area spanning the
331 boundary of Butte and Tehama counties, whereas *M. guttatus* distribution was predicted to
332 occur more broadly across the study area (Fig. 1A). The first principal component of the 22
333 modelled environmental variables explained over half of the variation observed and was
334 positively associated with elevation and bioclimatic variables indicative of precipitation
335 during dry and warm seasons, and negatively associated with bioclimatic variables explaining
336 variation in temperature. PC 2 explained nearly 20% of the observed variation and was
337 positively associated with temperature range variables and negatively associated with several
338 precipitation variables (Fig. 1C). *Mimulus guttatus* and *M. glaucescens* differed in their mean
339 position along PC1 (t = -5.93, df = 246.5, P < 0.001) for predicted occurrence points, but not
340 PC2 (t = -0.407, df = 279.8, P = 0.68).

341

342 Reproductive isolation

343 With the exception of ecogeographic isolation, the barriers to reproduction measured
344 provided modest or no contribution to reproductive isolation between species (Fig. 2,
345 Supplementary Methods and Results). For both species, the confidence intervals of

346 reproductive isolation overlapped zero for a majority of potential barriers (Table S3), and two
347 barriers for each species were significantly negative, indicating that hybrid matings
348 outperformed conspecific ones for these barriers. Total isolation was estimated to be
349 incomplete for both species, but higher for *M. glaucescens* (Fig. 2, *M. glaucescens* total RI
350 95% CI = 0.350-0.913; *M. guttatus* = 0.024-0.755), suggesting asymmetry in the strength of
351 isolation. Other than ecogeographic isolation, flowering phenology (both pre- and post-
352 zygotic) was the only barrier that was significantly positive for both species (Fig. 2).
353 Between-population estimates of reproductive isolation within each species were also weak
354 or overlapping zero, and broadly similar to between-species estimates (Table S3).
355
356 Genomic analyses
357 The complex phylogenetic history within *Simiolus* section of *Mimulus* reported
358 elsewhere (Swegart et al. 2008; Brandvain et al. 2014; Twyford & Friedman 2015; Coughlan
359 2020; Coughlan 2021) was re-confirmed (Fig. 3A). The widespread taxon *M. guttatus*
360 included deep genetic structure distinguishing a Northern and Southern clade, as has been
361 reported elsewhere (Brandvain et al. 2014; Twyford & Friedman 2015), whereas most other
362 named taxa included in the phylogeny represented monophyletic clades sister to one or both
363 of the two *M. guttatus* clades. This was also the case for *M. glaucescens*, which emerged as
364 monophyletic and sister to the Northern *M. guttatus* clade (Fig. 3A), although that monophyly
365 was not reciprocal for Northern *M. guttatus* (similar patterns appear elsewhere within the
366 phylogeny: Fig. 3A). Moreover, *M. glaucescens* appears to be one of the most recently
367 diverged taxa, with both a shorter branch length and relatively lower F_{ST} and D_{XY} compared
368 to other species pairs in the complex (Fig. 3C).
369 The first principal component of the genome-wide data within *M. glaucescens* and *M.*
370 *guttatus* mirrored the phylogenetic structure for Northern and Southern *M. guttatus* clades, in

371 that the accessions for the two clades clustered on different ends of that axis (Fig. 3B). The
372 second principal component, however, revealed distinct ancestry between *M. glaucescens*
373 from *M. guttatus*, with two Northern *M. guttatus* accessions clustering with all *M.*
374 *glaucescens* genomes. These two accessions had a majority (78% and 87%) of genomic
375 ancestry characteristic of *M. glaucescens* (Fig. 3D), and were from two populations within
376 the Butte Creek canyon area of local sympatry (Table S1). Although the ancestry percentages
377 in these two accessions were high and were responsible for breaking reciprocal monophyly
378 between Northern *M. glaucescens* and *M. guttatus* (Fig. 3A), *M. glaucescens*-like ancestry
379 was relatively common across *M. guttatus* accessions (mean *M. glaucescens*-like ancestry
380 was 24% and 10% for the Northern and Southern clade of *M. guttatus*, respectively; Fig. 3D).
381 The reverse, however, was not observed; *M. guttatus*-like ancestry was far lower within *M.*
382 *glaucescens* accessions (chiefly within sympatric accessions), consistent with the asymmetry
383 in reproductive isolation observed (Fig. 2).

384 Several lines of evidence suggested recent or ongoing introgression between *M.*
385 *glaucescens* and *M. guttatus*. *Mimulus glaucescens* and *M. guttatus* shared unusually low
386 differentiation and divergence compared to other pairs of taxa sampled (Fig. 3C, Table S5;
387 D_{XY} = 0.039 vs 0.043 for Northern vs. Southern *M. guttatus* clades, respectively). This result,
388 however, varied with distribution; differentiation and divergence were higher between
389 allopatric accessions of Northern *M. guttatus* and *M. glaucescens* vs. sympatric accessions
390 (allopatric: D_{XY} = 0.0399, F_{ST} = 0.1090; sympatric: D_{XY} = 0.0351, F_{ST} = 0.0037), suggesting a
391 history of introgression in sympatry. Similarly, Patterson's D revealed significantly higher
392 introgression between sympatric accessions than allopatric accessions of *M. glaucescens* and
393 Northern *M. guttatus* (Fig. 4). Overall, introgression appeared to be common between both
394 clades of *M. guttatus* and *M. glaucescens*, particularly for Northern *M. guttatus* in close
395 proximity to *M. glaucescens.*

396

397 DISCUSSION

398

399 Speciation presupposes robust barriers to gene flow (Mayr 1942; Coyne and Orr
400 2004), thus well-defined species with less than robust isolation provoke consternation. The
401 taxa considered herein, *Mimulus guttatus* and *M. glaucescens*, have distinctive vegetative
402 morphology (Fig. 1B) that has led generations of taxonomists (Greene 1885; Grant 1924;
403 Hickman 1993; Baldwin et al. 2012; Barker et al. 2012; Nesom 2012) to place them into
404 separate species, despite nomenclatural instability in close relatives (e.g., Barker et al. 2012;
405 Nesom 2012), and even within *M. guttatus* (Grant 1924; Nesom 2012). The morphological
406 traits distinguishing *M. glaucescens* from *M. guttatus* are not reported as intermediate forms
407 in the field (C.T. Ivey, personal observation) or herbaria (Nesom 2012, but see Vickery
408 1964). Despite divergent phenotypes, our estimates of reproductive isolation between these
409 taxa were low (Fig. 2), with only a couple of barriers estimated to be stronger between
410 species than between populations within a species (Table S3). Genomic evidence underscored
411 the idea that species boundaries were porous. Allopatric accessions had greater genetic
412 divergence, but regardless of distribution, weak genetic differentiation and significant
413 introgression was observed between *M. glaucescens* and *M. guttatus* (Fig. 4). Overall, *M.*
414 *glaucescens* should perhaps be regarded as an incipient species or an ecotype of *M. guttatus*,
415 despite over a century of stable taxonomic status as a distinct species.

416 The notion that reproductively isolated or otherwise genetically distinct taxa could
417 experience routine gene flow was historically controversial but has been widely reported
418 more recently (Mebert 2008; Fitzpatrick et al. 2008; Martin et al. 2013; Harrison and Larson
419 2014; Gao et al. 2020; Jiao and Yang 2020). Persistent gene flow despite significant
420 reproductive barriers has been observed in diverse taxa (Fitzpatrick et al. 2008; Larson et al.

421 2014; Richards et al. 2018; Schield et al. 2019), including other monkeyflowers (Brandvain et
422 al. 2014; Kenny and Sweigart 2016; Nelson et al. 2021; Kiang and Hamrick 1978; Martin and
423 Willis 2007; Case and Willis 2008; Fishman et al. 2014; Kenny and Sweigart 2016;
424 Schemske and Bradshaw 1999; Ramsey et al. 2003). Speciation has been shown to proceed in
425 the face of gene flow in some cases (Martin et al. 2013; Harrison and Larson 2014). Our
426 results are thus consistent with an emerging understanding of speciation that admits that gene
427 flow can be a routine occurrence during speciation, particularly during its early stages.
428 Of course, reproductive barriers limit introgression for many taxa. Prezygotic barriers
429 are often considered to evolve more rapidly (Widmer et al. 2009; Baack et al. 2015; Christie
430 et al. 2022), but postzygotic reproductive isolation can also be important (DiVittorio et al.
431 2020; Coughlan and Matutue 2020; Sandstedt et al. 2021). Regardless, the environment often
432 mediates isolation, as with immigrant inviability (Nosil et al. 2005; Richards and Ortiz-
433 Barrientos 2016) or selection against ecologically-unfit hybrids (Jacquemyn et al. 2018;
434 Ferris and Willis 2018). For *M. glaucescens* and *M. guttatus*, the strongest barrier was
435 ecogeographic, with climate and elevation as potential agents of ecological differentiation
436 (Fig. 1). Ecogeographic isolation is often strong in plants (Lowry et al. 2008a, 2008b; Sobel
437 2014; Li et al. 2018; Christie & Strauss 2018; Vargas et al. 2020; Sianta and Kay 2021),
438 although divergence in habitat is often associated with genetically based differences in
439 reproductive biology, such as flowering time (Silvertown et al. 2005; Antonovics 2006;
440 Bomblies 2010; Sianta and Kay 2021) or pollination (Grossenbacher and Whittall 2011;
441 Ostevik et al. 2012). Otherwise, assortative mating within taxa may be limited, with free
442 genomic exchange, except for loci explicitly involved in local adaptation (e.g., Hendrick et al.
443 2016). In addition to ecogeographic isolation, we found significantly positive, though weak,
444 isolation based on divergence in flowering time (Fig. 2), which is consistent with the idea that
445 habitat and reproductive divergence may co-occur during speciation. Despite weak isolation,

446 the distinctive genetic coherence of *M. glaucescens* was supported based on the phylogenetic
447 analysis (Fig. 3) as well as estimates of differentiation; for example, D_{XY} between Northern
448 *M. guttatus* and *M. glauscens* was higher than π (nucleotide diversity) within Northern *M.*
449 *guttatus* (Fig. 3; Table S4).

450 The factors maintaining vegetative differences between *M. glaucescens* and *M.*
451 *guttatus* (Fig. 1) remain unclear. To our knowledge the genetic basis for expression of these
452 traits (peduncular bract fusion and glaucousness, trichomes) in *M. glaucescens* has not been
453 characterized, but large-effect QTL for glaucousness and trichome density reported from
454 other studies (Bennet et al. 2012; Holeski et al. 2010; Hendrick et al. 2016) suggest that
455 segregating phenotypes might not be intermediate. If so, hybrid or introgressed individuals
456 may be difficult to discern in the field based on vegetative phenotype alone. Glaucousness
457 has been found to facilitate drought tolerance (Xue et al. 2017) and defense against insect
458 herbivores (Eigenbrode and Espelie 1995). Similarly, transitions in trichome density have
459 been shown to be influenced by natural selection within other monkeyflower taxa (Hendrick
460 et al. 2016). The extent to which these traits contribute to the divergence observed in habitat
461 distribution between *M. glaucescens* and *M. guttatus* remains to be tested.

462 The pattern of distribution observed – asymmetric range sizes, broadly sympatric, but
463 with environmentally based geographic divergence – was similar to that reported for other
464 pairs of *Mimulus* sister taxa (Grossenbacher et al. 2014; Sobel 2014) and indeed, pairs of
465 sister taxa more generally within the California Floristic Province (Anacker and Strauss
466 2014). This pattern is not inconsistent with models of budding (or peripatric) speciation
467 (Grossenbacher et al. 2014). The genomic analyses are also consistent with the idea that
468 budding speciation is common throughout the species complex; many of the taxa included in
469 the phylogeny, including *M. glaucescens*, were sister to one of the main *M. guttatus* clades

470 (Fig. 3A). Similarly, *M. guttatus* ancestral variation was substantially represented within each
471 of the putatively derived taxa (Fig. 3A; Fig. S1; Table S5).

472 In conclusion, we show that the recently diverged, but well differentiated taxa, *M.*
473 *glaucescens* and *M. guttatus*, have surprisingly low reproductive isolation and abundant gene
474 flow, in contrast to what is suggested by their taxonomy and morphology. This study
475 contributes to a growing understanding of the complex evolutionary patterns involved in the
476 formation of species boundaries during speciation (Martin et al. 2013; Feder et al. 2014;
477 Harrison and Larson 2014; Jiao and Yang 2020; Stankowski and Ravinet 2021; Coughlan et
478 al. 2021) and the contribution of reproductive barriers toward delineation of lineages (Baack
479 et al. 2015; Ostevik et al. 2016; Christie and Strauss 2019; Runemark et al. 2019). More
480 fundamentally, these results underscore that integration of classical ecological studies of
481 reproductive isolation with genomic approaches will be instrumental for continued progress
482 in disentangling this fundamental and intriguing evolutionary process.

483

484 REFERENCES

485

486 Anacker BL, Strauss SY. 2014. The geography and ecology of plant speciation: range overlap
487 and niche divergence in sister species. Proceedings of the Royal Society B 281: 20132980.
488
489 Antonovics J. 2006. Evolution in closely adjacent plant populations X: long-term persistence
490 of prereproductive isolation at a mine boundary. Heredity 97: 33-37.
491
492 Baack E, Melo MC, Rieseberg LH, Ortiz-Barrientos D. 2015. The origins of reproductive
493 isolation in plants. New Phytologist 207: 968-984.
494
495 Baldwin BG, Goldman DH, Keil DJ, Patterson R, Rosatti TJ, Wilken DH (eds.). 2012. The
496 Jepson manual: vascular plants of California, second edition. University of California Press,
497 Berkeley, CA.
498
499 Barker WR, Nesom GL, Beardsley PM, Fraga NS. 2012. A taxonomic conspectus of
500 Phrymaceae: a narrowed circumscription for *Mimulus*, new and resurrected genera, and new
501 names and combinations. Phytoneuron 39: 1-60.
502
503 Beardsley PM, Schoenig SE, Whittall JB, Olmstead RG. 2004. Patterns of evolution in
504 western North American *Mimulus* (Phrymaceae). American Journal of Botany 91: 474-489.

Bennett D, Izanloo A, Edwards J, Kuchel H, Chalmers K, Tester M, Reyonolds M, Schnurbusch T, Langridge P. 2012. Identification of novel quantitative trait loci for days to ear emergence and flag leaf glaucouseness in a bread wheat (*Triticum aestivum* L.) population adapted to southern Australian conditions. Theoretical and Applied Genetics 124: 697-711.

Bomblies K. 2010. Doomed lovers: mechanisms of isolation and incompatibility in plants. Annual Review of Plant Biology 61: 109-124.

Brandvain Y, Kenney AM, Flagel L, Coop G, Sweigart AL. 2014. Speciation and introgression between *Mimulus nasutus* and *Mimulus guttatus*. PLOS Genetics 106: e1004410.

Carr DE, Dudash MR. 1997. The effects of five generations of enforced selfing on potential male and female function in *Mimulus guttatus*. Evolution 51: 1797-1807.

Case AL, Willis JH. 2008. Hybrid male sterility in *Mimulus* (Phrymaceae) is associated with a geographically restricted mitochondrial rearrangement. Evolution 62: 1026-1039.

Christie K, Strauss SY. 2018. Along the speciation continuum: quantifying intrinsic and extrinsic isolating barriers across five million years of evolutionary divergence in California jewelflowers. Evolution 72: 1063-1079.

Christie K, Strauss SY. 2019. Reproductive isolation and the maintenance of species boundaries in two serpentine endemic jewelflowers. Evolution 73: 1375-1391.

Christie K, Fraser LS, Lowry DB. 2022. The strength of reproductive isolating barriers in seed plants: insights from studies quantifying premating and postmating reproductive barriers over the past 15 years. Evolution https://doi.org/10.1111/evo.14565

Coughlan JM, Matute DR. 2020. The importance of intrinsic postzygotic barriers throughout the speciation process. Philosophical Transactions of the Royal Society B 375: 20190533.

Coughlan JM, Brown MW, Willis JH. 2020. Patterns of hybrid seed inviability in the *Mimulus guttatus* sp. complex reveal a potential role of parental conflict in reproductive isolation. Current Biology 30: 83-93.

Coughlan JM, Brown MW, Willis JH. 2021. The genetic architecture and evolution of life-history divergence among perennials in the *Mimulus guttatus* species complex. Proceedings of the Royal Society B 288: 20210077.

Coyne JA, Orr HA. 1989. Patterns of speciation in *Drosophila*. Evolution 43: 362-381.

549 Coyne JA, Orr HA. 2004. Speciation. Sinauer Associates, Sunderland, MA.
550
551 DiVittorio CT, Singhal S, Roddy AB, Zapata F, Ackerly DD, Baldwin BG, Brodersen CR,
552 Búrquez A, Fine PVA, Flores MP, Solis E, Morales-Villavicencio J, Morales-Arce D, Kyhos
553 DW. 2020. Natural selection maintains species despite frequent hybridization in the desert
554 shrub *Encelia*. Proceedings of the National Academy of Sciences USA 117: 33373-33383.
555
556 De La Torre AR, Roberts DR, Aitken SN. 2014. Genome-wide admixture and ecological
557 niche modelling reveal the maintenance of species boundaries despite long history of
558 interspecific gene flow. Molecular Ecology 23: 2046-2059.
559
560 Eigenbrode SD, Espelie KE. 1995. Effects of plant epicuticular lipids on insect herbivores.
561 Annual Review of Entomology 40: 171-194.
562
563 Feder JL, Nosil P, Wacholder AC, Egan SP, Berlocher SH, Flaxman SM. 2014. Genome-
564 wide congealing and rapid transitions across the speciation continuum during speciation with
565 gene flow. Journal of Heredity 105: 810-820.
566
567 Ferris KG, Willis JH. 2018. Differential adaptation to a harsh granite outcrop habitat between
568 sympatric *Mimulus* species. Evolution 72: 1225-1241.
569
570 Ferris KG, Sexton JP, Willis JH. 2014. Speciation on a local geographic scale: the evolution
571 of a rare rock outcrop specialist in *Mimulus*. Philosophical Transactions of the Royal Society
572 B 369: 20140001.
573
574 Fishman L, Sweigart AL, Kenny AM, Campbell S. 2014. Major quantitative trait loci control
575 divergence in critical photoperiod for flowering between selfing and outcrossing species of
576 monkeyflower (*Mimulus*). New Phytologist 201: 1498-1507.
577
578 Fitzpatrick BM, Placyk Jr. JS, Niemiller ML, Casper GS, Burghardt GM. 2008.
579 Distinctiveness in the face of gene flow: hybridization between specialist and generalist
580 gartersnakes. Molecular Ecology 17: 4107-4117.
581
582 Gao Y, Harris AJ, Li H, Gao X. 2020. Hybrid speciation and introgression both underlie the
583 genetic structures and evolutionary relationships of three morphologically distinct species of
584 *Lilium* (Liliaceae) forming a hybrid zone along an elevational gradient. Frontiers in Plant
585 Science 11: 576407.
586
587 Grant AL. 1924. A monograph of the genus *Mimulus*. Annals of the Missouri Botanical
588 Garden 11: 99-389.
589
590 Greene EL. 1885. Studies in the botany of California and parts adjacent. Bulletin of the
591 California Academy of Sciences 1: 66-127.
592

593 Grossenbacher DL, Whittall JB. 2011. Increased floral divergence in sympatric
594 monkeyflowers. Evolution 65: 2712-2718.
595
596 Grossenbacher DL, Veloz SD, Sexton JP. 2014. Niche and range size patterns suggest that
597 speciation begins in small, ecologically diverged populations in North American
598 monkeyflowers (*Mimulus* spp.). Evolution 68: 1270-1280.
599
600 Harrison RG, Larson EL. 2014. Hybridization, introgression, and the nature of species
601 boundaries. Journal of Heredity 105: 795-809.
602
603 Hendrick MF, Finseth FR, Mathiasson ME, Palmer KA, Broder EM, Breigenzer P, Fishman
604 L. 2016. The genetics of extreme microgeographic adaptation: an integrated approach
605 identifies a major gene underlying leaf trichome divergence in Yellowstone *Mimulus*
606 *guttatus*. Molecular Ecology 25: 5647-5662.
607
608 Hickman JC (ed.). 1993. The Jepson Manual. University of California Press, Berkeley, CA.
609
610 Holeski LM, Chase-Alone R, Kelly JK. 2010. The genetics of phenotypic plasticity in plant
611 defense: trichome production in *Mimulus guttatus*. American Naturalist 175: 391-400.
612
613 Ivey CT, Carr DE. 2012. Tests for the joint evolution of mating system and drought escape in
614 *Mimulus*. Annals of Botany 109: 583-598.
615
616 Jacquemyn H, De Kort H, Broeck AV, Brys R. 2018. Immigrant and extrinsic hybrid seed
617 inviability contribute to reproductive isolation between forest and dune ecotypes of *Epipactis*
618 *helleborine* (Orchidaceae). Oikos 127: 73-84.
619
620 Jiao X, Yang Z. 2021. Defining species when there is gene flow. Systematic Biology 70: 108-
621 119.
622
623 Joffard N, Silva WTAF, Twyford AD. 2021. The role of postzygotic isolation in *Mimulus*
624 speciation. Evolution 75: 756-758.
625
626 Kay KM. 2006. Reproductive isolation between two closely related hummingbird-pollinated
627 neotropical gingers. Evolution 60: 538-552.
628
629 Kenney AM, Sweigart AL. 2016. Reproductive isolation and introgression between
630 sympatric *Mimulus* species. Molecular Ecology 25: 2499-2517.
631
632 Kiang YT, Hamrick JL. 1978. Reproductive isolation in the *Mimulus guttatus-M. nasutus*
633 complex. American Midland Naturalist 100: 269-276.
634

Kopelman NM, Mayzel, J, Jakobsson M, Rosenberg NA, Mayrose I. 2015. CLUMPAK: a program for identifying clustering modes and packaging population structure inferences across *K*. Molecular Ecology Resources 15: 1179-1191.

Korneliussen TS, Albrechtsen A, Nielsen R. 2014. ANGSD: analysis of next generation sequencing data. BMC Bioinformatics 15: 356.

Korunes KL, Samuk K. 2021. PIXY: Unbiased estimation of nucleotide diversity and divergence in the presence of missing data. Molecular Ecology Resources 21: 1359-1368.

Larson EL, White TA, Ross CL, Harrison RG. 2014. Gene flow and the maintenance of species boundaries. Molecular Ecology 23: 1668-1678.

Li Q, Grossenbacher DL, Angert AL. 2018. The effect of range overlap on ecological niche divergence depends on spatial scale in monkeyflowers. Evolution 72: 2100-2113.

Lowry DB, Modliszewski JL, Wright KM, Wu CA, Willis JH. 2008a. The strength and genetic basis of reproductive isolating barriers in flowering plants. Philosophical Transactions of the Royal Society B 363: 3009-3021.

Lowry DB, Rockwood RC, Willis JH. 2008b. Ecological reproductive isolation of coast and inland races of *Mimulus guttatus*. Evolution 62: 2196-2214.

Lowry DB, Sobel JM, Angert AL, Ashman T-L, Baker RL, Blackman BK, Brandvain Y, Byers KJRP, Cooley AM, Coughlan JM, Dudash MR, Fenster CB, Ferris KG, Fishman L, Friedman J, Grossenbacher DL, Holeski LM, Ivey CT, Kay KM, Koelling VA, Kooyers NJ, Murren CJ, Muir CD, Nelson TC, Peterson ML, Puzey JR, Rotter MC, Seemann JR, Sexton JP, Sheth SN, Streisfeld MA, Sweigart AL, Twyford AD, Vallejo-Marín M, Willis JH, Wright KM, Wu CA, Yuan Y-W. 2019. The case for the continued use of the genus name *Mimulus* for all monkeyflowers. Taxon 68: 617-623.

Malinsky M, Matschiner M, Svardal H. 2021. Dsuite-Fast *D*-statistics and related admixture evidence from VCF files. Molecular Ecology Resources 21: 584-595.

Martin NH, Willis JH. 2007. Ecological divergence associated with mating system causes nearly complete reproductive isolation between sympatric *Mimulus* species. Evolution 61: 68-82.

Martin SH, Dasmahapatra KK, Nadeau NJ, Salazar C, Walters JR, Simpson F, Blaxter M, Manica A, Mallet J, Jiggins CD. 2013. Genome-wide evidence for speciation with gene flow in *Heliconius* butterflies. Genome Research 23: 1817-1828.

Mayr E. 1942. Systematics and the origin of species. Columbia University Press, New York, NY.

Mebert K. 2008. Good species despite massive hybridization: genetic research on the contact zone between the watersnakes *Nerodia sipedon* and *N. fasciata* in the Carolinas, USA. Molecular Ecology 17: 1918-1929.

Merrill RM, Gompert Z, Dembeck LM, Kronforst MR, McMillan WO, Jiggins CD. 2011. Mate preference across the speciation continuum in a clade of mimetic butterflies. Evolution 65: 1489-1500.

Moyle LC, Olson MS, Tiffin P. 2004. Patterns of reproductive isolation in three angiosperm genera. Evolution 58: 1195-1208.

Munz PA. 1959. A California flora. University of California Press, Berkeley, CA.

Nelson TC, Stathos AM, Vanderpool DD, Finseth FR, Yuan Y-W, Fishman L. 2021. Ancient and recent introgression shape the evolutionary history of pollinator adaptation and speciation in a model monkeyflower radiation (*Mimulus* section Erythranthe). PLOS Genetics 17: 1009095.

Nesom GL. 2012. Taxonomy of *Erythranthe* sect. Simiola (Phrymaceae) in the USA and Mexico. Phytoneuron 40:1-123.

Nguyen L-T, Schmidt HA, von Haeseler A, Minh BQ. 2015. IQ-TREE: a fast and effective stochastic algorithm for estimating maximum-likelihood phylogenies. Molecular Biology and Evolution 32: 268–74.

Nosil P, Vines TH, Funk DJ. 2005. Reproductive isolation caused by natural selection against immigrants from divergent habitats. Evolution 59: 705-719.

Ostevik KL, Moyers BT, Owens GL, Rieseberg LH. 2012. Parallel ecological speciation in plants? International Journal of Ecology 2012: 939862.

Ostevik KL, Andrew RL, Otto SP, Rieseberg LH. 2016. Multiple reproductive barriers separate recently diverged sunflower ecotypes. Evolution 70: 2322-2335.

Owens GL, Rieseberg LH. 2013. Hybrid incompatibility is acquired faster in annual than in perennial species of sunflower and tarweed. Evolution 68: 893-900.

Powell TH, Hood GR, Murphy MO, Heilveil JS, Berlocher SH, Nosil P, Feder JL. 2013. Genetic divergence along the speciation continuum: the transition from host race to species in *Rhagoletis* (Diptera: Tephritidae). Evolution 67: 2561-2576.

Puzey JR, Willis JH, Kelly JK. 2017. Population structure and local selection yield high genomic variation in *Mimulus guttatus*. Molecular Ecology 26: 519-535.

Ramsey J, Bradshaw Jr., HD, Schemske DW. 2003. Components of reproductive isolation between the monkeyflowers *Mimulus lewisii* and *M. cardinalis* (Phrymaceae). Evolution 57: 1520-1534.

Richards TJ, Ortiz-Barrientos D. 2016. Immigrant inviability produces a strong barrier to gene flow between parapatric ecotypes of *Senecio lautus*. Evolution 70: 1239-1248.

Richards EJ, Poelstra JW, Martin CH. 2018. Don't throw out the sympatric speciation with the crater lake water: fine-scale investigation of introgression provides equivocal support for causal role of secondary gene flow in one of the clearest examples of sympatric speciation. Evolution Letters 2: 524-540.

Ritland C, Ritland K. 1989. Variation of sex allocation among eight taxa of the *Mimulus* guttatus species complex (Scrophulariaceae). American Journal of Botany 76: 1731-1739.

Runemark A, Vallejo-Marin M, Meier JI. 2019. Eukaryote hybrid genomes. PLOS Genetics 15: e1008404.

Sambatti JBM, Strasburg JL, Ortiz-Barrientos D, Baack EJ, Rieseberg LH. 2012. Reconciling extremely strong barriers with high levels of gene exchange in annual sunflowers. Evolution 66: 1459-1473.

Sandstedt GD, Wu CA, Sweigart AL. 2021. Evolution of multiple postzygotic barriers between species of the *Mimulus tilingiii* complex. Evolution 75: 600-613.

Schemske DW, Bradshaw Jr. HD. 1999. Pollinator preference and the evolution of floral traits in monkeyflowers (*Mimulus*). Proceedings of the National Academy of Sciences 96: 11910-11915.

Schield DR, Perry BW, Adams RH, Card DC, Jezkova T, Pasquesi GIM, Nikolakis ZL, Row K, Meik JM, Smith CF, Mackessy SP, Castoe TA. 2019. Allopatric divergence and secondary contact with gene flow: a recurring theme in rattlesnake speciation. Biological Journal of the Linnean Society 128: 149-169.

Selby JP, Willis JH. 2018. Major QTL controls adaptation to serpentine soils in *Mimulus guttatus*. Molecular Ecology 27: 5073-5087.

Servedio MR, Kirkpatrick M. 1997. The effects of gene flow on reinforcement. Evolution 51: 1764-1772.

Sianta SA, Kay KM. 2021. Parallel evolution of phenological isolation across the speciation continuum in serpentine-adapted annual wildflowers. Proceedings of the Royal Society B 288: 20203076.

Silvertown J, Servaes C, Biss P, Macleod D. 2005. Reinforcement of reproductive isolation between adjacent populations in the Park Grass Experiment. Heredity 95: 198-205.

Skotte L, Korneliussen TS, Albrechtsen A. 2013. Estimating individual admixture proportions from next generation sequencing data. Genetics 195: 693-702.

Sobel JM. 2014. Ecogeographic isolation and speciation in the genus *Mimulus*. American Naturalist 184: 565-579.

Sobel JM, Chen GF. 2014. Unification of methods for estimating the strength of reproductive isolation. Evolution 68: 1511-1522.

Stankowski S, Ravinet M. 2021. Defining the speciation continuum. Evolution 75: 1256-1273.

Sweigart AL, Willis JH. 2003. Patterns of nucleotide diversity in two species of *Mimulus* are affected by mating system and asymmetric introgression. Evolution 57: 2490-2506.

Sweigart AL, Martin NH, Willis JH. 2008. Patterns of nucleotide variation and reproductive isolation between a *Mimulus* allotetraploid and its progenitor species. Molecular Ecology 17: 2089-2100.

Twyford AD, Friedman J. 2015. Adaptive divergence in the monkey flower *Mimulus guttatus* is maintained by a chromosomal inversion. Evolution 69: 1476-1486.

Twyford AD, Streisfeld MA, Lowry DB, Friedman J. 2015. Genomic studies on the nature of species: adaptation and speciation in *Mimulus*. Molecular Ecology 24: 2601-2609.

Vargas OM, Goldston B, Grossenbacher DL, Kay KM. 2020. Patterns of speciation are similar across mountainous and lowland regions for a neotropical plant radiation (Costaceae: *Costus*). Evolution 74: 2644-2661.

Via S. 2009. Natural selection in action during speciation. Proceedings of the National Academy of Sciences USA. 106: 9939-9946.

Vickery Jr. RK. 1964. Barriers to gene exchange between members of the *Mimulus guttatus* complex (Scrophulariaceae). Evolution 18: 52-69.

Vickery Jr. RK. 1978. Case studies in the evolution of species complexes in *Mimulus* Evolutionary Biology 11: 405-507.

Widmer A, Lexer C, Cozzolino S. 2009. Evolution of reproductive isolation in plants. Heredity 102: 31-38.

Wu CA, Lowry DB, Cooley AM, Wright KM, Lee YW, Willis JH. 2008. *Mimulus* is an emerging model system for the integration of ecological and genomic studies. Heredity 100: 220-230.

Xue D, Zhang X, Lu X, Chen G, Chen ZH. 2017. Molecular and evolutionary mechanisms of cuticular wax for plant drought tolerance. Frontiers in Plant Science 8: 621.

Zinkl GM, Zwiebel BI, Grier DG, Preuss D. 1999. Polen-stigma adhesion in Arabidopsis: a species-specific interaction mediated by lipophilic molecules in the pollen exine. Development 126: 5431-5440.

Figure captions:

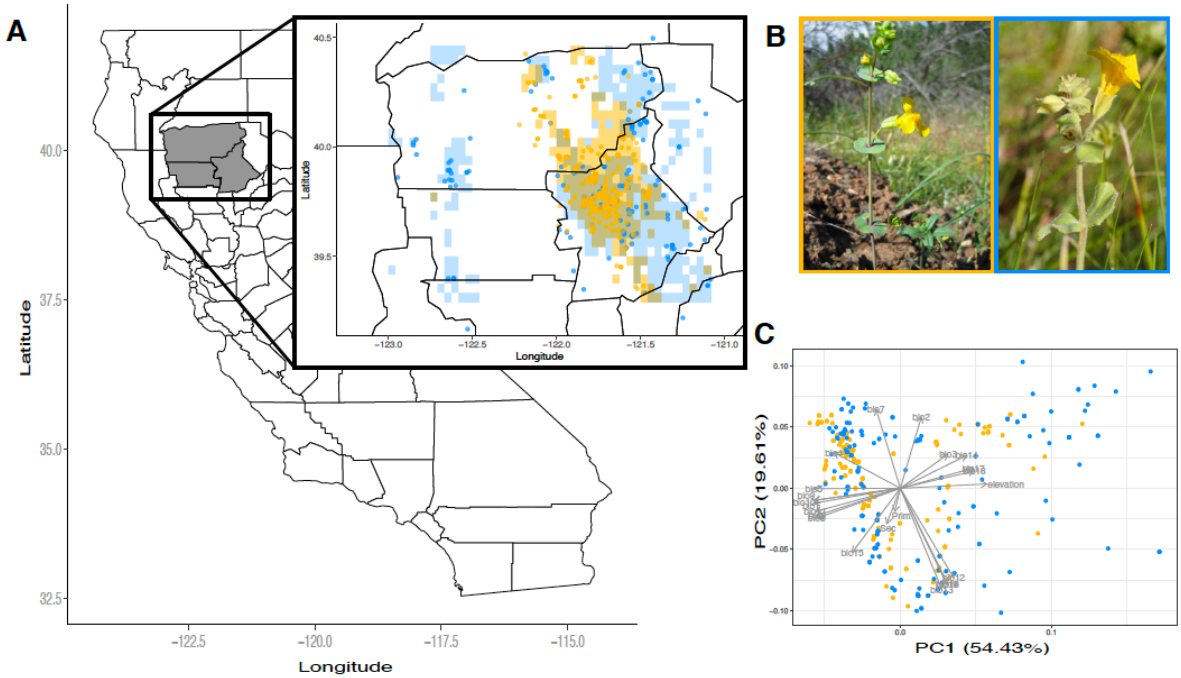

Figure 1: Geographic distributions of *Mimulus glaucescens* and *M. guttatus*. (A) State of California with focal counties in gray; inset: predicted local ranges of *M. guttatus* (blue) and *M. glaucescens* (yellow) based on maxent modeling. Points represent collection records upon which the models are based. (B) *M. glaucescens* (left) and *M. guttatus* (right), showing distinct vegetative morphology, (C) PCA based on 19 Bioclim variables, elevation, and two soil substrate variables used to build the maxent models.

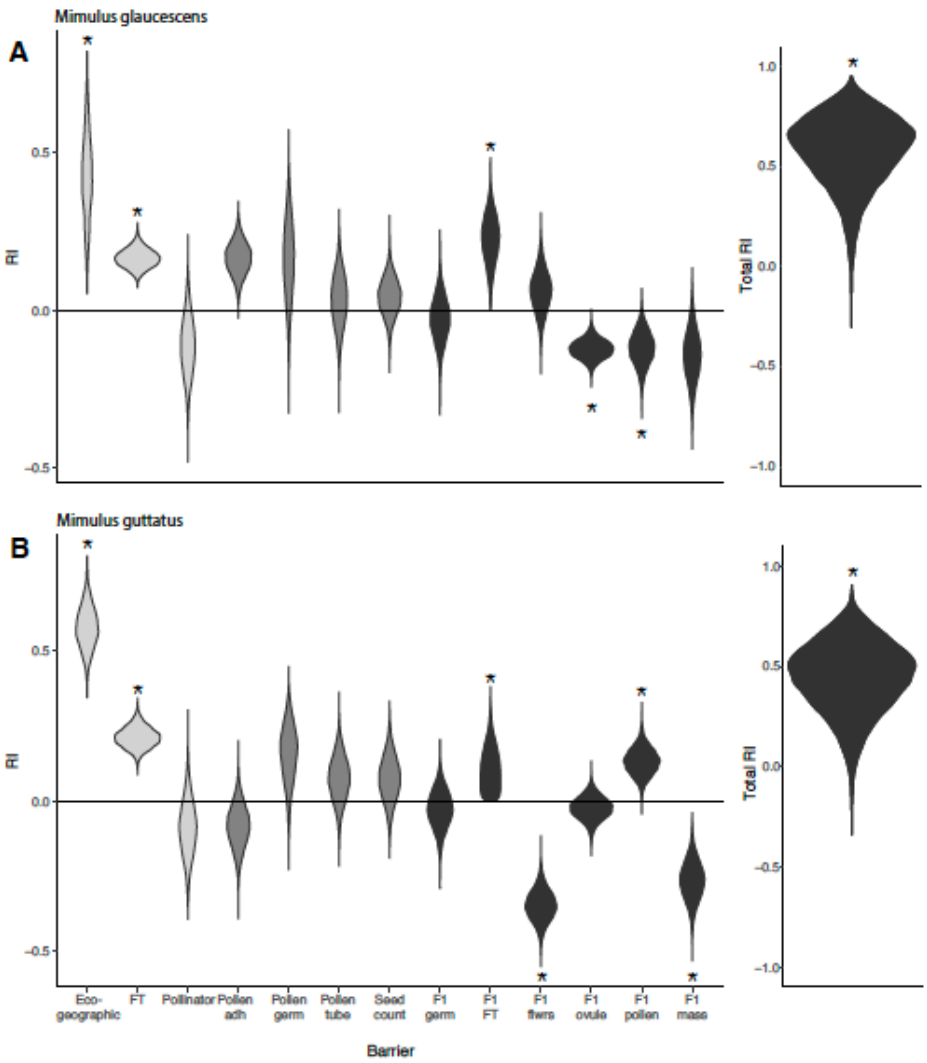

Fig. 2: Reproductive isolation for *M. glaucescens* (A) and *M. guttatus* (B). Distributions based on 10,000 bootstrapped values (ecogeographic is based on 1000). Shadings represent types of barriers pale gray = premating barriers, dark gray = postmating, prezygotic barriers, black = postzygotic barriers. Asterisks indicate estimates with 95% CI that do not overlap 0 (Table S5).

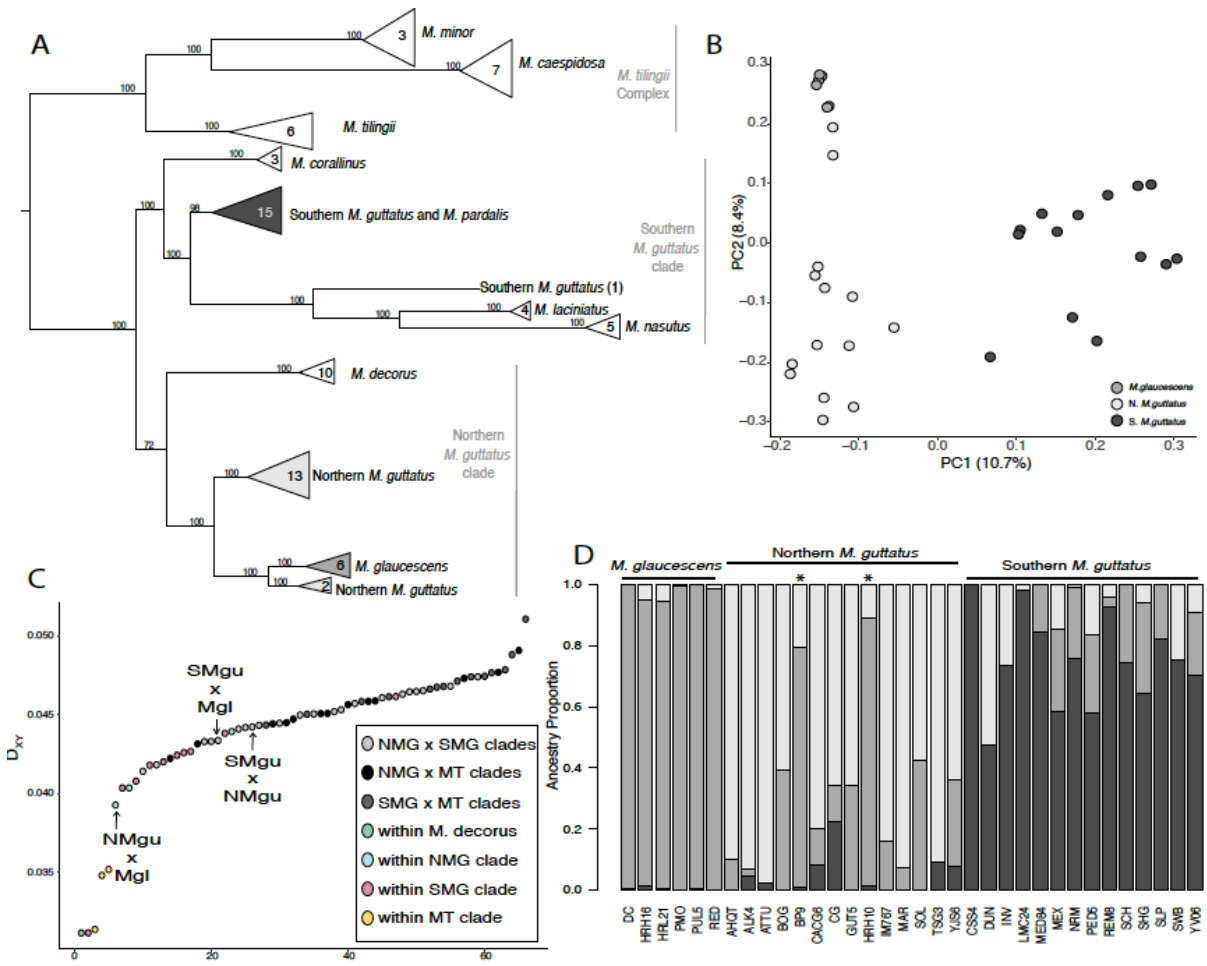

Figure 3. (A) Maximum-likelihood phylogeny of sampled *Mimulus* taxa based on 75 whole-genome sequences, with *M. dentilobus* (not shown) as an outgroup. Number of accessions is shown at tips next to each taxon name. (B) First two principal components of genomic variation in *Mimulus guttatus* (Southern and Northern clades represented in black and pale gray, respectively) and *M. glaucescens* (dark gray). (C) Divergence (D_{XY}) in genomic variation in pairs of accessions of *Mimulus*, arranged in increasing order of D_{XY}. Mean D_{XY} between selected taxa indicated by arrows (see also Table S4). NMG = Northern *M. guttatus*; SMG = Southern *M. guttatus*; MT = *M. tillingii*; Mgl = *M. glaucescens*. (D) Proportion of genome associated with ancestry of *M. glaucescens* (dark gray), Northern *M. guttatus* (light gray), and Southern *M. guttatus* (black) taxa for accessions sampled in study (see also Table S3), based on a K-means clustering analysis (see text). Asterisks indicate *M. guttatus* samples collected from within an area of sympatry with *M. glaucescens*.

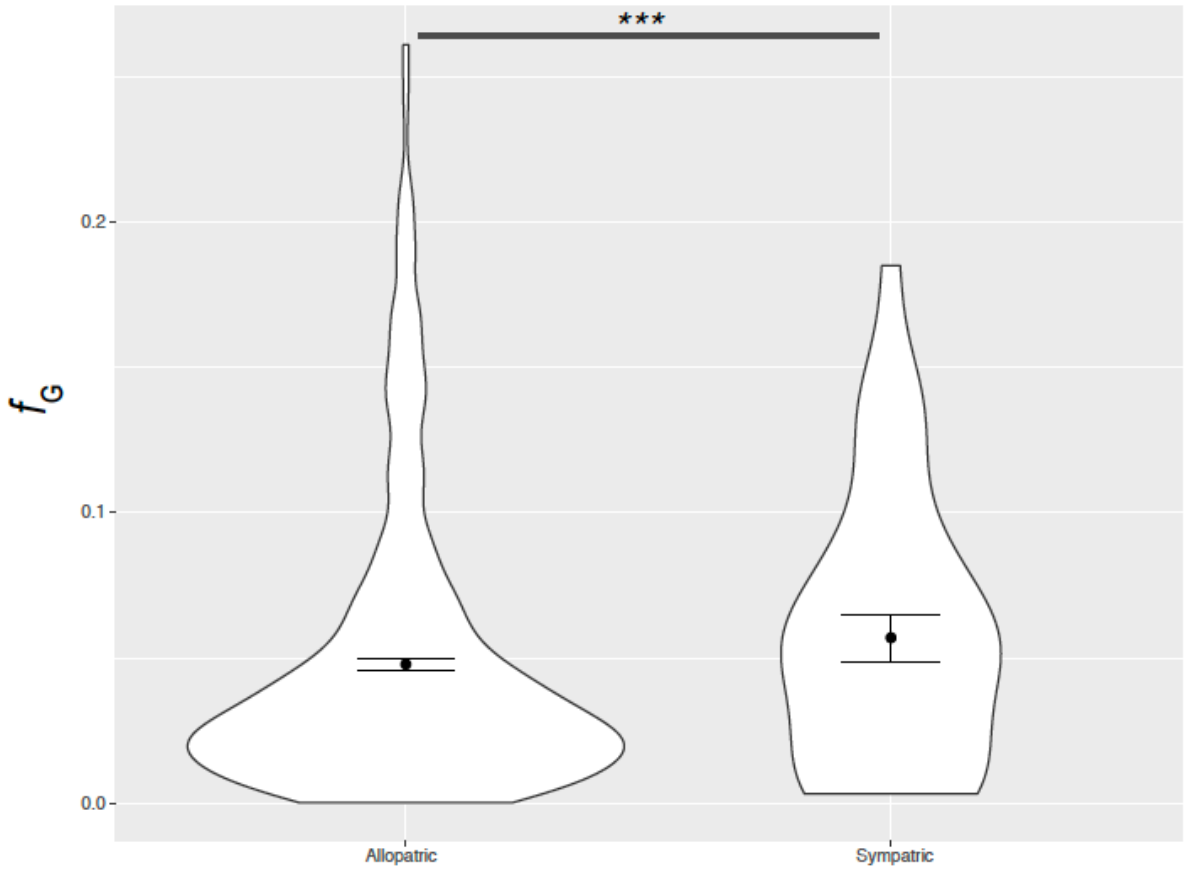

856

857 Fig. 4. Violin plots of jack-knifed estimates of fraction of admixture (f_G) in *M. glaucescens*

858 and Northern *M. guttatus* accessions with allopatric or sympatric distributions. Estimates of

859 f_G were significantly higher from sympatric accessions (χ^2=91.2, df=1, p<0.0001).

860

861

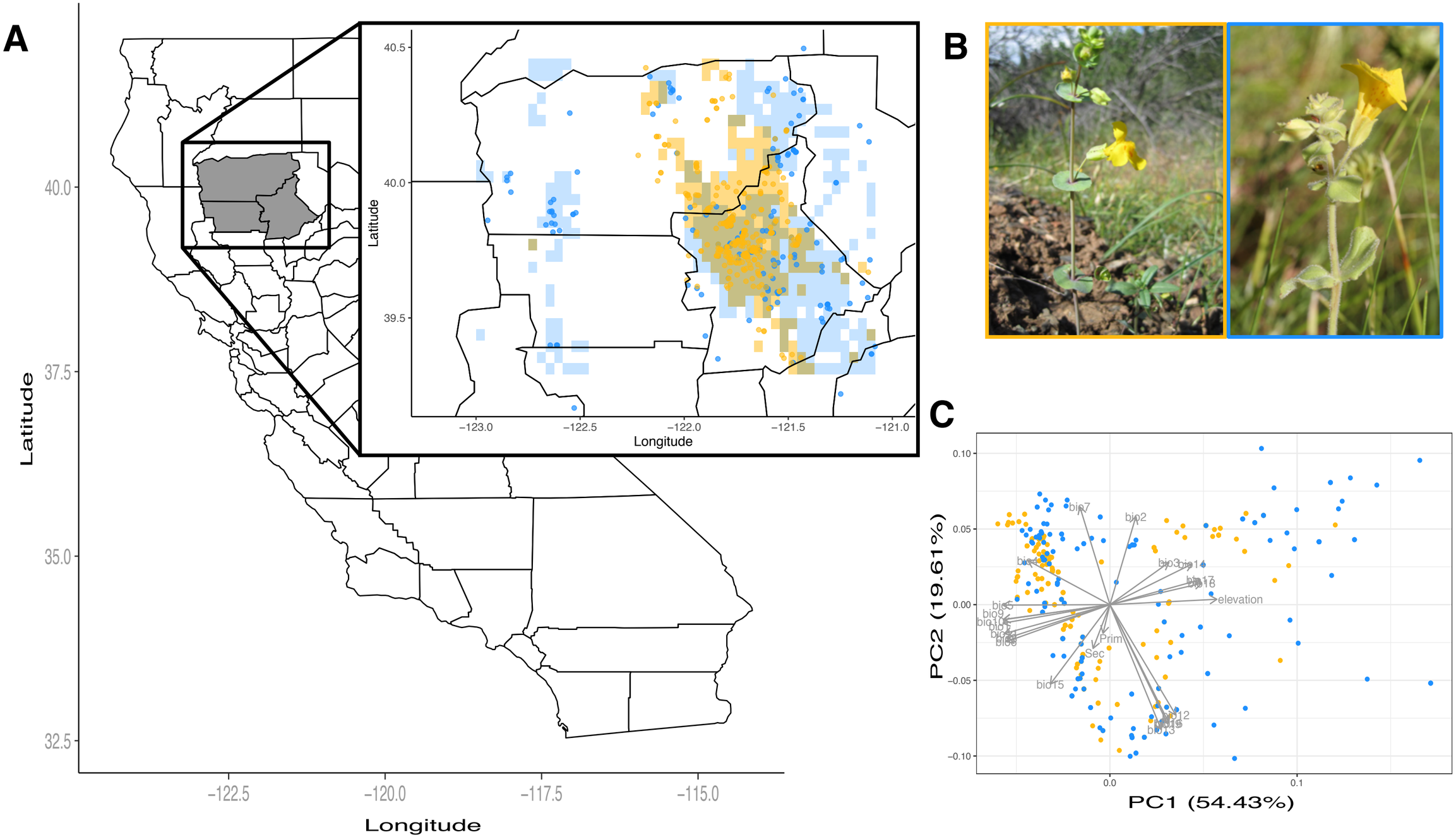
A
B
C
Latitude
Longitude
40.0
37.5
35.0
32.5
−122.5
−120.0
−117.5
−115.0
40.5
40.0
39.5
−123.0
−122.5
−122.0
−121.5
−121.0
PC1 (54.43%)
PC2 (19.61%)
0.10
0.05
0.00
−0.05
−0.10
0.0
0.1
bio7
bio2
bio3
bio14
bio17
bio18
elevation
bio5
bio9
bio10
bio6
bio8
Prim
Sec
bio15
bio12
bio13

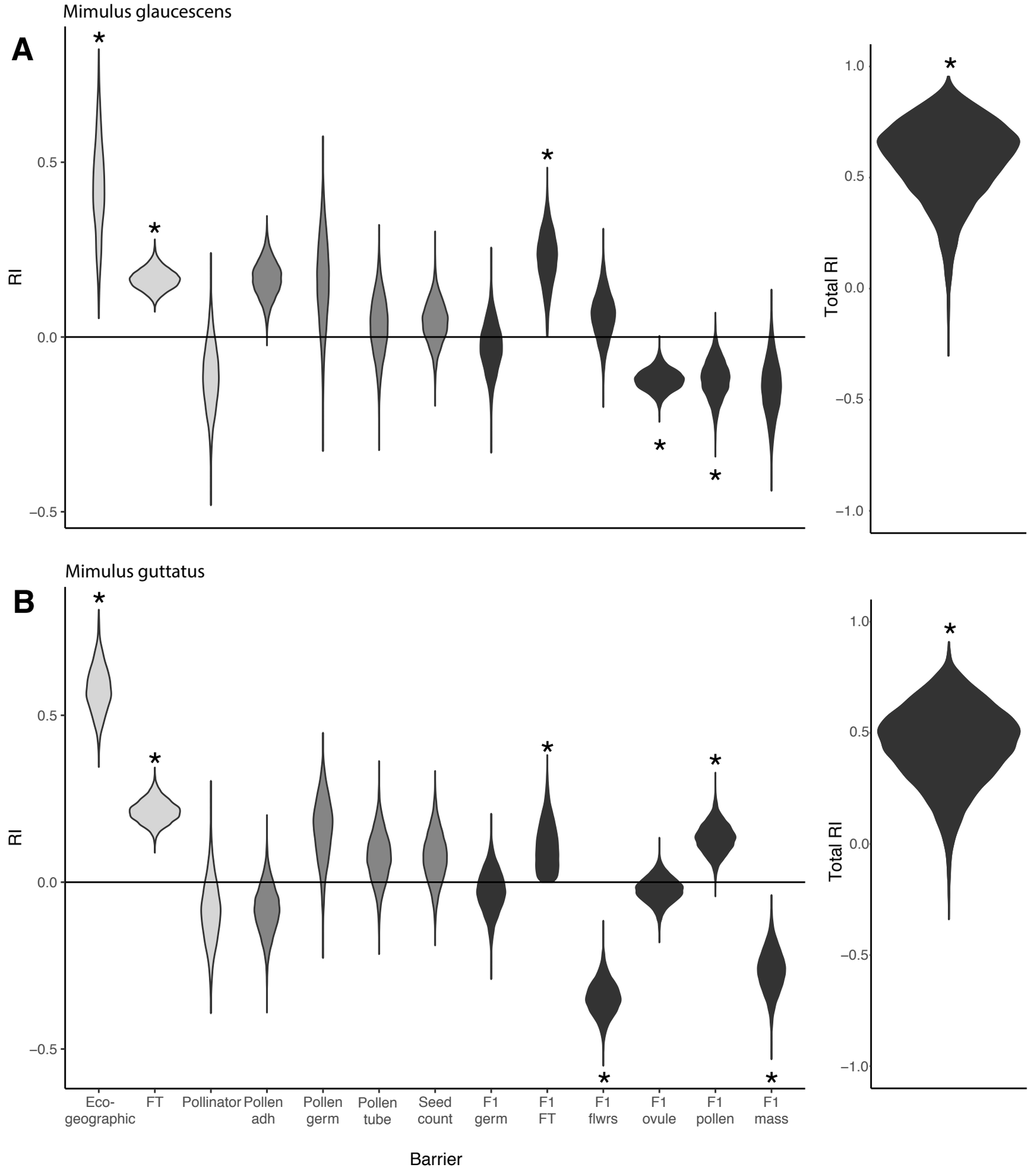
Mimulus glaucescens
A
RI
0.5
0.0
−0.5
Total RI
1.0
0.5
0.0
−0.5
−1.0
Mimulus guttatus
B
RI
0.5
0.0
−0.5
Total RI
1.0
0.5
0.0
−0.5
−1.0
Eco-geographic
FT
Pollinator
Pollen adh
Pollen germ
Pollen tube
Seed count
F1 germ
F1 FT
F1 flwrs
F1 ovule
F1 pollen
F1 mass
Barrier

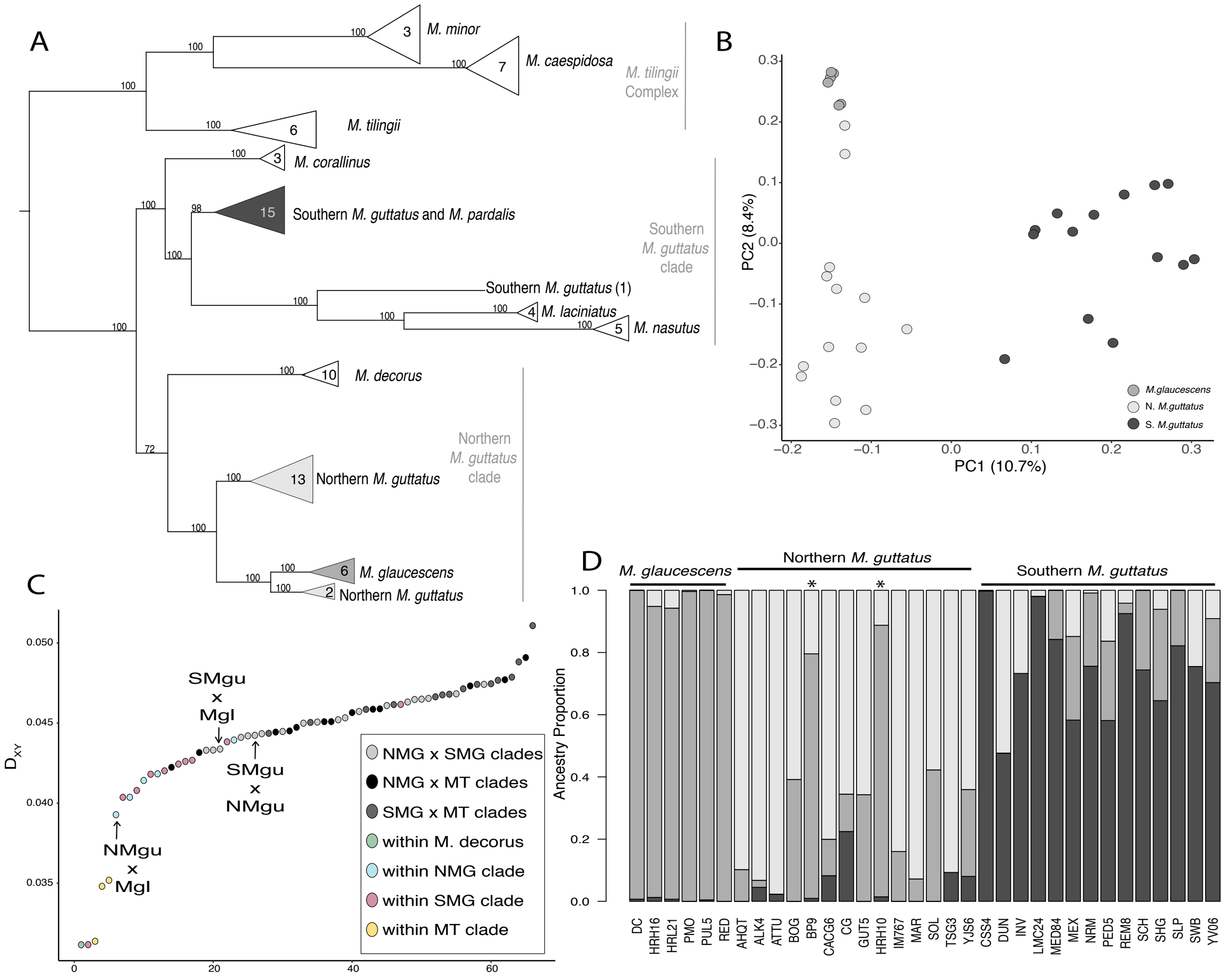
A
M. minor
M. caespidosa
M. tilingii Complex
M. tilingii
M. corallinus
Southern M. guttatus and M. pardalis
Southern M. guttatus (1)
M. laciniatus
M. nasutus
Southern M. guttatus clade
M. decorus
Northern M. guttatus
M. glaucescens
Northern M. guttatus
Northern M. guttatus clade
B
PC2 (8.4%)
PC1 (10.7%)
M.glaucescens
N. M.guttatus
S. M.guttatus
C
D_XY
SMgu x Mgl
SMgu x NMgu
NMgu x Mgl
NMG x SMG clades
NMG x MT clades
SMG x MT clades
within M. decorus
within NMG clade
within SMG clade
within MT clade
D
M. glaucescens
Northern M. guttatus
Southern M. guttatus
Ancestry Proportion
DC HRH16 HRL21 PMO PUL5 RED AHQT ALK4 ATTU BOG BP9 CACG6 CG GUT5 HRH10 IM767 MAR SOL TSG3 YJS6 CSS4 DUN INV LMC24 MED84 MEX NRM PED5 REM8 SCH SHG SLP SWB YV06

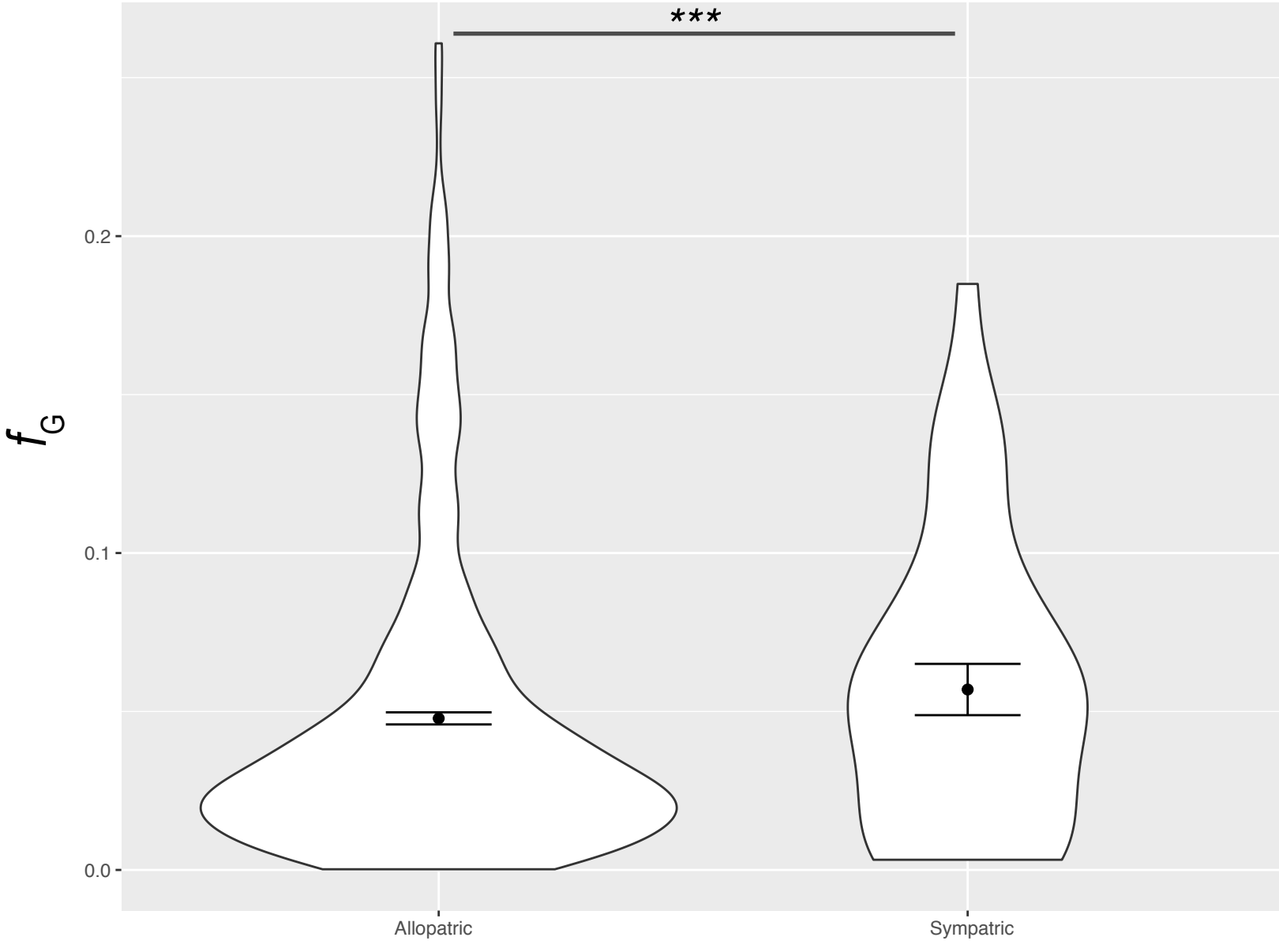
***
0.2
0.1
0.0
f_G
Allopatric
Sympatric